

# Adaptive Centralized Protection Scheme for Microgrids Based on Positive Sequence Complex Power

S. B. A. Bukhari, R. Haider, M. S. Zaman, Y. S. Oh, G. J. Cho, M. S. Kim, J. S. Kim, C. H. Kim

**Abstract--** Microgrids are regarded as an appropriate way to integrate the distributed generations in the distribution networks. Microgrids can operate in either the grid-tied mode or the standalone mode. Microgrids face many technical challenges; protection of microgrids is one of them. In this paper, we propose a new centralized protection scheme for microgrids based on positive sequence complex power. The phasor measurement units (PMUs) extract and communicate the fault information from each end of the line to a microgrid protection commander (MPC). The MPC processes the received data to detect, locate and isolate the faults in microgrids. The fault incidents are detected based on the mode of operation of microgrids. After the fault detection, fault bus identification (FBI) and fault line identification (FLI) algorithms are triggered to identify the faulty line in microgrids. Finally, a trip signal is sent to the relevant circuit breakers to isolate the faulty part.

**Keywords:** Microgrid, Adaptive protection, Fault Detection, Fault Location.

## I. INTRODUCTION

THE integration of low and medium voltage distributed generation (DG) in the distribution networks has been increasing due to the benefits such as reduced greenhouse emission, improved power quality, loss reduction and high efficiency. To achieve maximum benefits, the DGs are usually integrated in the distribution networks as a microgrid [1]. A microgrid is a small network that has various DGs, energy storage devices and electrical/heat loads. It can operate in either the grid-tied mode or the standalone mode. Microgrids provide high-quality power and increase the reliability for the end-users who need uninterruptible power supply.

Notwithstanding various advantages offered by microgrids, they may pose protection and control challenges, which need to be explored. The problem related to the microgrid protection arises due to 1) the presence of looped feeder 2) bidirectional power flow and 3) reduced fault current level in the standalone mode due to the limited current carrying capacity of power electronics devices [2]. The fault current is

clamped to 2-3 p.u of the rated current in case of inverter based DGs.

The traditional overcurrent relays are not appropriate for the protection of microgrids because they works on the assumptions of high fault current, radial structure and single mode operation. Although it is possible to use the overcurrent relays for the protection of grid-tied microgrids, the existing relay settings should be carefully revised as the existence of DGs may compromise the protection coordination.

A protection scheme for microgrid should take into account all these aforementioned issues. Researchers have developed various schemes to protect the microgrids. A summary of schemes is given in [3], [4]. The existing microgrid protection schemes can be divided into three categories: 1) local measurement based schemes, 2) communication based schemes and 3) protection using external devices. The local measurement based schemes use locally measured voltage and current signals to protect the microgrids. In [5], the voltage magnitude was used to identify the faults, and in [2], the overcurrent relays were used to protect the microgrids. The schemes did not require any communication link. The authors in [6] used wavelet packet transform for the coordination of digital relays to detect and clear the faults in microgrids. The local measurement based schemes are cheap but cannot guarantee the protection in both modes of operation. Moreover, the schemes are suitable for only one mode of operation either the grid-tied mode or the standalone mode. On the other hand, the communication based schemes exchange information among relays and/or central processing unit to protect the microgrids. In [7], the relay settings were computed centrally and updated in accordance with the change in status of the microgrid by using communication channel between the overcurrent relays and central processing unit. In [8], the communication link was proposed among overcurrent relays to detect and isolate the faults in microgrids. In [9], the voltage and currents signals from both ends of each line were communicated to a central processing unit where the protection functions were performed. Various differential protections schemes were proposed in [10], [11]. These schemes used time synchronised measurement to protect the microgrid. The external devices were used to equalise the fault current level in both the grid-tied and the standalone modes of microgrid [12]. The fault current limiters or energy storage devices were usually used as external devices for the protection of microgrids. These schemes were impractical because they required significant investment.

---

This work was supported by the National Research Foundation of Korea (NRF) grant funded by the Korea government (MSIP) (No. 2015R1A2A1A10052459).

The authors are with the College of Information and Communication Engineering, Sungkyunkwan University, Suwon City, 440-746, South Korea (E-mail: s.basit41@skku.edu; razahaider@skku.edu; saeed568@skku.edu; fivebal2@naver.com; thug1220@naver.com; lovelykiku25@naver.com; kjs7107@naver.com; chkim@skku.edu ).

Paper submitted to the International Conference on Power Systems Transients (IPST2017) in Seoul, Republic of Korea June 26-29, 2017

This paper proposes a new centralized protection scheme for microgrids based on positive sequence complex power. The PMUs at each end of a microgrid line extract and communicate the voltage and current signals to the microgrid protection commander (MPC). The main protection functions i.e. fault detection, fault location and trip signal generation are accomplished in the MPC. The fault incidents are detected based on the operating mode of microgrids. After the fault detection, a fault bus identification (FBI) algorithm is initiated to identify the three buses close to the fault point. A fault line identification (FLI) scheme is then applied on all lines connected to the buses (selected by FBI) to identify the faulty line. Finally, the MPC sends trip signals to the relevant circuit breakers to isolate the faulty line from the microgrid.

## II. MICROGRID TEST SYSTEM

To explain and test the proposed scheme, a microgrid shown in Fig. 1 is considered. The network and load data of the test system are given in Table I and Table II respectively. The microgrid consists of two photovoltaic systems of 2MW each and a wind system of 3MW. The DGs are interfaced with the network through a 0.63/12.47KV transformer. A droop based voltage/frequency regulation scheme is used in this study for all DGs [13]. The microgrid can be operated in the standalone mode by opening the switches S1 and S2. The switch S3 is closed during the standalone operation to maintain the generation load balance in the microgrid.

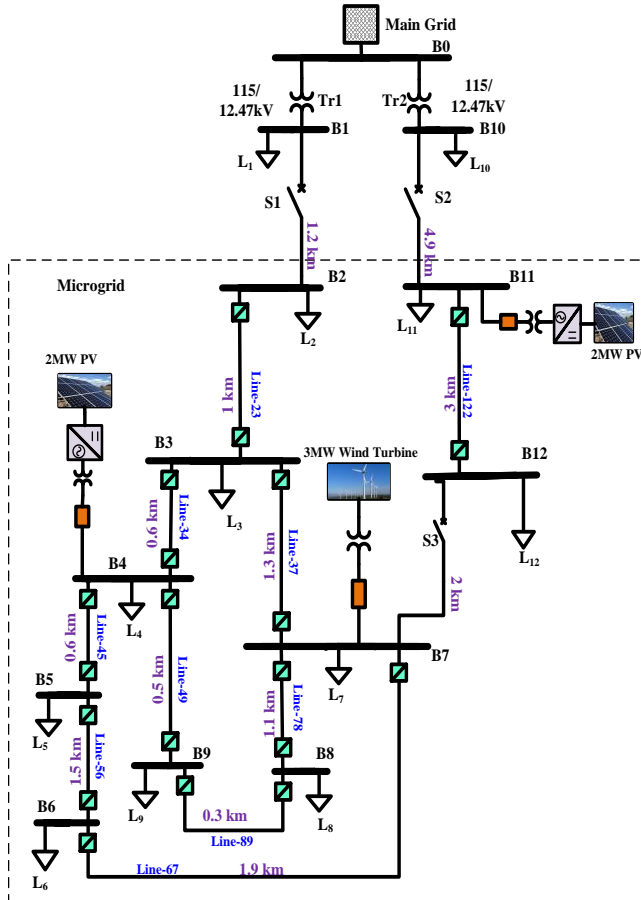


Fig. 1. Single line diagram of microgrid test system.

TABLE I  
DISTRIBUTION LINE PARAMETERS

Parameter	Value
Positive-Sequence Series Impedance	0.173+j0.432 $\Omega$ /Km
Positive-Sequence Shunt Susceptance	3.831 $\mu\text{S}$ /Km
Zero-Sequence Series Impedance	0.351+j1.8 $\Omega$ /Km
Zero-Sequence Shunt Susceptance	1.57 $\mu\text{S}$ /Km

TABLE II  
PARAMETERS OF LOADS AT EACH BUS

Load	Phase A		Phase B		Phase C	
	KW	KVAr	KW	KVAr	KW	KVAr
L <sub>1</sub>	7330	3355	6802	3072	6652	3154
L <sub>2</sub>	265	136	302	173	445	220
L <sub>3</sub>	64	48	244	135	109	69
L <sub>4</sub>	180	87	90	43	90	43
L <sub>5</sub>	232	88	170	53	42	26
L <sub>6</sub>	47	15	95	31	258	93
L <sub>7</sub>	95	31	190	62	95	31
L <sub>8</sub>	90	43	135	65	180	87
L <sub>9</sub>	95	31	142	46	95	31
L <sub>10</sub>	2050	1083	2050	1083	2050	1083
L <sub>11</sub>	175	94	175	94	127	79
L <sub>12</sub>	191	134	191	134	191	134

## III. PROPOSED PROTECTION SCHEME

The proposed protection strategy is developed based on data communication from the PMUs to the MPC. The PMUs installed at each bus extract the voltage and current phasors and transfer them to the MPC. The MPC receives and processes the signals to detect and locate the fault in the microgrids. Once the fault is located, the MPC recognises the faulty phase and issues the trip signals to relevant circuit breakers to isolate the faulty line from rest of the microgrid. The following subsections describe the methods used in the proposed strategy to achieve the protection goals.

### A. Detection of Fault Incidents

To detect various faults in the microgrid, this paper uses adaptive fault detection strategy. The proposed fault detection strategy depends on the mode of operation of microgrids. In the grid-tied mode, the utility grid also contributes to fault current, so the fault currents are significantly large. Therefore, the overcurrent relays are adequate to detect the fault in the grid-tied microgrid. On the other hand, the fault currents are relatively small in the standalone mode due to the presence of inverter based DGs in the system. Therefore, the use of overcurrent relays is ineffective to detect the faults in the standalone microgrid. However, a fault within the standalone microgrid causes a network-wide voltage drop, which can be used to detect the fault incidents. Thus, this study uses under voltage relays to detect the fault incident in the standalone microgrids.

### B. Fault Location

To increase the reliability and to maintain the continuity of supply to healthy parts of power system, it is necessary to locate the faults accurately. In this paper, the fault location is determined in two steps. Firstly, the FBI algorithm determines three buses close to the fault point. The FLI algorithm is then applied on all lines connected to the selected buses to find the exact faulted line. The following subsections explain the steps

in detail.

### 1) Fault Bus Identification:

The FBI algorithm uses magnitude of positive sequence voltage (PSV) to determine the buses close to the fault point. The distribution of magnitude of the positive sequence voltage from the source to load is shown in Fig. 2. According to Fig. 2, the PSV magnitude is maximum at source points and it is minimum at fault point. Therefore, the bus with minimum PSV magnitude can be regarded as the closest bus to the faulted line. Hence, the PSV magnitude of two buses at both ends of the faulted line are minimum among the voltages of other buses in the microgrid. The PSV magnitudes of all the buses are ranked in increasing order to determine suspected bus. It is possible to locate the faulted line by selecting only one bus. However, the proposed scheme may mal-operate in some situation like the occurrence of same minimum PSV magnitude at two buses. Moreover, the measurement error may also affect the proposed scheme. To overcome these issues and to increase the reliability and selectivity of proposed scheme, the three buses corresponding to top three values of PSV magnitude are selected as the buses near to fault point. Selecting more than three buses increase the computational complexity of proposed scheme.

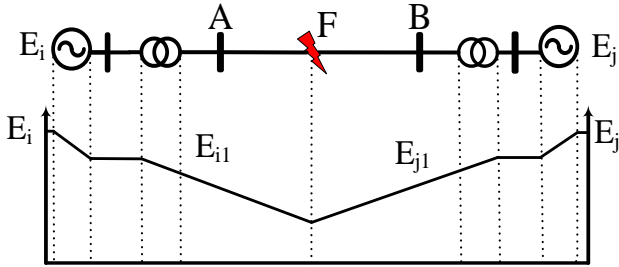


Fig. 2. Distribution of PSV in a faulted power system.

### 2) Fault Line Identification:

To understand the FLI algorithm, Line-34 of the microgrid shown in Fig. 1 is considered. The equivalent circuit of this line can be obtained by replacing the upstream and downstream of the line by their equivalent impedances along with equivalent voltage sources as shown in Fig. 3 [9]. Faults F1 and F2 represent the forward and reverse faults with respect to the PMU-34 of the microgrid respectively.

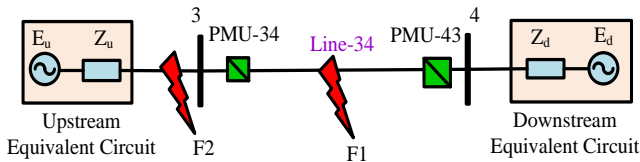


Fig. 3. Equivalent circuit of Line-34 of the microgrid.

**Internal Faults:** The sequence networks diagram for fault F1, which is an internal fault for the protection of the Line-34, is shown in Fig. 4a. The switches are closed based on the fault type. To develop a general model for the analysis of various

fault, the equivalent impedance can replace the zero and negative sequence impedances. The resultant equivalent circuit for fault F1 is shown in Fig. 4b. In the Fig. 4b,  $Z_{eq2,0,f}$  represents the equivalent impedance of negative and zero sequence networks along with the fault impedance.

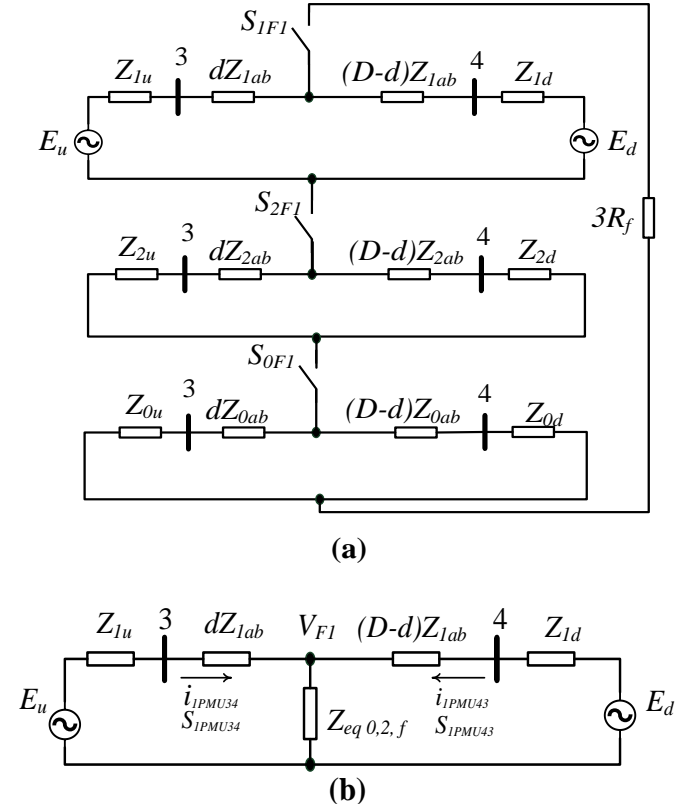


Fig. 4. (a). Sequence network of Line-34 of the microgrid. (b). Generalised sequence network of Line-34 for fault F1.

Assuming the positive direction of electrical quantities from the bus to the line, the positive sequence current flowing through PMU34 can be calculated as:

$$i_{1PMU34} = \frac{E_u - V_{F1}}{Z_{1u} + dZ_{1ab}} \quad (1)$$

Where  $Z_{1u}$ ,  $Z_{1ab}$  represent the positive sequence impedances of the upstream network and Line-34 respectively, while  $V_{F1}$  is the voltage at fault point F1. The positive sequence complex power at PMU34 is given as:

$$S_{1PMU34} = i_{1PMU34}^2 \times Z_{1u} \quad (2)$$

$$S_{1PMU34} = \left( \frac{E_u - V_{F1}}{Z_{1u} + dZ_{1ab}} \right)^2 \times Z_{1u} \quad (3)$$

Similarly, the positive sequence complex power at PMU-43 can be computed as:

$$S_{1PMU43} = \left( \frac{E_d - V_{F1}}{Z_{1d} + (D-d)Z_{1ab}} \right)^2 \times Z_{1d} \quad (4)$$

Where  $Z_{1d}$  represents the positive sequence impedance of downstream network.

A new FLI coefficient based on the positive sequence complex power is developed to differentiate between the faulty and the healthy lines. The FLI coefficient is given as follows:

$$K_{34} = \frac{|S_{1PMU34} + S_{1PMU43}|}{|S_{1PMU34} - S_{1PMU43}|} \quad (5)$$

In case of internal faults, the complex power flows from the bus to the line. Therefore, the sum of  $S_{1PMU34}$  and  $S_{1PMU43}$  will be greater than their difference. Hence, for an internal fault, the FLI coefficient takes a value greater than 1.

**External Faults:** Fig. 5 shows the generalised sequence network of the Line-34 during the external fault F2.

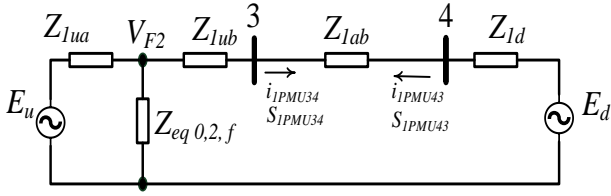


Fig. 5. Generalised sequence network of Line-34 for fault F2.

The positive sequence current flowing from the PMU34 and PMU43 can be computed as:

$$i_{1PMU34} = -i_{1PMU43} = -\frac{E_d - V_{F2}}{Z_{1d} + Z_{1ab} + Z_{1ub}} \quad (6)$$

Where  $Z_{1ub}$  represents the positive sequence impedance between fault point and bus 3,  $V_{F2}$  is the voltage at fault point F2 and  $Z_{1d}$  denotes the positive sequence impedance of downstream equivalent circuit.

The positive sequence complex power at PMU34 is as follows:

$$S_{1PMU34} = -i_{1PMU34}^2 \times (Z_{1d} + Z_{1ab}) \quad (7)$$

$$S_{1PMU43} = -\left( \frac{E_d - V_{F2}}{Z_{1d} + Z_{1ab} + Z_{1ub}} \right)^2 \times (Z_{1d} + Z_{1ab}) \quad (8)$$

Similarly, the positive sequence complex power at PMU-43 will be

$$S_{1PMU43} = \left( \frac{E_d - V_{F2}}{Z_{1d} + Z_{1ab} + Z_{1ub}} \right)^2 \times Z_{1d} \quad (9)$$

$$K_{34} = \frac{|S_{1PMU34} + S_{1PMU43}|}{|S_{1PMU34} - S_{1PMU43}|} \quad (10)$$

In case of external faults, the sum of  $S_{1PMU34}$  and  $S_{1PMU43}$  will be less than their difference because the positive sequence complex power flows in positive direction at bus 4 while it flows in negative direction at bus 3. Hence, the value of the FLI coefficient is less than 1 for external faults.

### C. Fault Phase Identification

The proposed scheme uses positive sequence components in the FBI and FLI algorithms to identify the faulty line in the microgrids. The calculation of positive sequence components involves all the three phases. Therefore, it is not possible to recognise the faulty phase by using these algorithms. To retain the single phase tripping capability of proposed scheme, a fault classification algorithm is added in the MPC. The algorithm takes help from the adaptive fault detection strategy to identify the faulty phase. The MPC considers a phase as faulty when the overcurrent or under voltage relay associated with that phase detects the fault. The fault classification strategy along with trip signal generation is shown in Fig. 6. In Fig. 6, the number '50' and '27' represent the overcurrent and under voltage relays respectively. Finally, based on the fault type, the MPC generates and sends trip signals to the relevant circuit breaker to isolate the faulty line from rest of the microgrid. If the breaker fails to isolate the fault in a timely manner, a backup trip signal will be sent to the neighbouring circuit breaker.

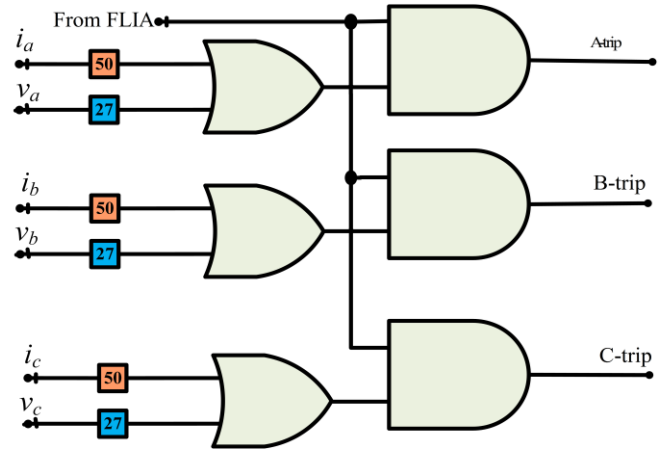


Fig. 6. Fault phase identification logic.

## IV. SIMULATION STUDIES

To validate the efficacy of proposed scheme, extensive simulations were carried out using MATLAB/SIMULINK software package. The test system used in this study is shown in Fig. 1. The simulations were performed for all ten types of faults at various locations in the microgrid. The performance of proposed scheme is tested under the grid-tied and the standalone mode of operation. The communication delay is taken as 2 ms while the time taken by PMU to process and

send data to MPC is taken as 25ms.

### A. Standalone Mode of Operation

Let us consider that a three-phase fault hits the Line-56 of the microgrid in the standalone mode of operation. The positive sequence voltage magnitude at various buses during the fault is shown in Fig. 7. The PSV at all buses is close to 1 p.u before the occurrence of fault. The PSV magnitude changes when the fault occurs at the Line-56 of the microgrid. The three buses with minimum PSV magnitude are 6, 5 and 4 respectively. Five lines are connected to these three buses. Fig. 8 shows the corresponding FLI coefficients of the lines along with the current at PMU56. It can be observed from Fig. 8 that the FLI coefficient of Line-56 is greater than 1 while the FLI coefficients for all other lines connected to the buses 4, 5 and 6 are less than 1. The proposed scheme identifies the faulty line after some delay. The delay is because the PMUs and MPC require some time to process the signals. Table III reports the results for various faults at different location in the microgrid. The FLI coefficients of faulty line are written in bold letters. It is clear from Table III that the FLI coefficients are greater than one for faulted line and less than one for healthy line.

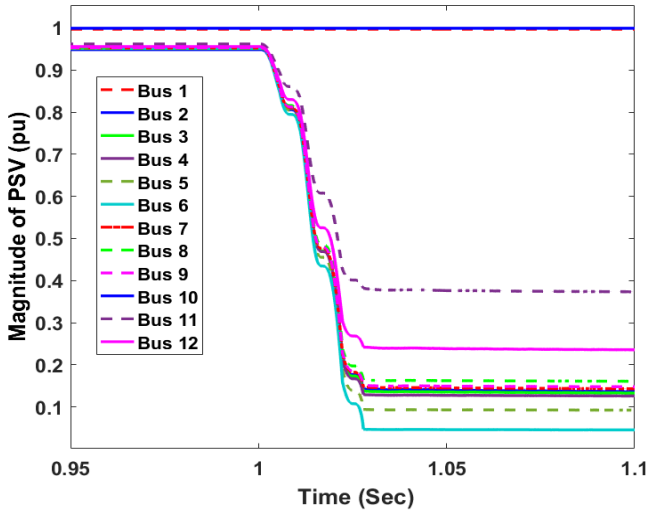


Fig. 7. Magnitude of PSVs at various buses when fault occurs at Line-56 of the standalone microgrid.

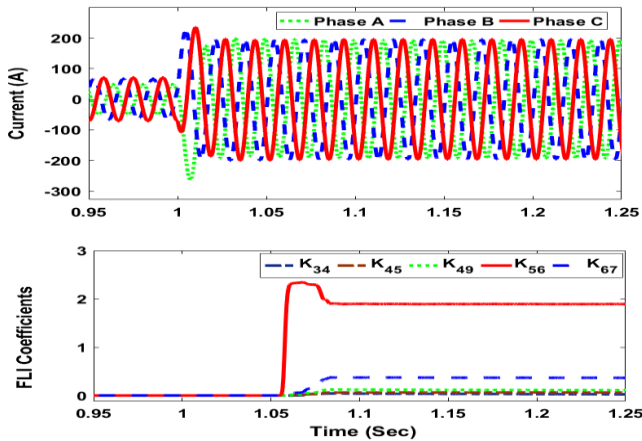


Fig. 8. Current signal at PMU56 and FLI coefficients for three-phase fault at line-56 of the standalone microgrid.

TABLE III

RESULTS FOR VARIOUS KIND OF FAULTS AT DIFFERENT LOCATIONS IN THE MICROGRID WORKING IN THE STANDALONE MODE

Fault Location	Fault Type	FBI	K <sub>xy</sub> for the lines connected to the selected Buses		
			Bus-A	Bus-B	Bus-C
Line-49	CG	B2, B4, B9	K <sub>12</sub> =0.06 K <sub>23</sub> =0.09	K <sub>43</sub> =0.044 K <sub>45</sub> =0.051 <b>K<sub>49</sub>=13.5</b>	K <sub>98</sub> =9e-3, <b>K<sub>94</sub>=13.6</b>
Line-37	BG	B2, B3, B7	K <sub>12</sub> =0.089 K <sub>23</sub> =0.075	K <sub>23</sub> =0.081 <b>K<sub>37</sub>=9.31</b> K <sub>34</sub> =0.087	K <sub>76</sub> =0.054 <b>K<sub>73</sub>=9.41</b> K <sub>78</sub> =0.085
Line-128	BCG	B6, B7, B12	K <sub>56</sub> =0.068 K <sub>67</sub> =0.092	K <sub>67</sub> =0.088 K <sub>73</sub> =0.075 <b>K<sub>128</sub>=2.4</b>	<b>K<sub>128</sub>=2.37</b> K <sub>112</sub> =0.08
Line-67	ABC	B6, B7, B12	K <sub>56</sub> =0.062 <b>K<sub>67</sub>=4.15</b>	K <sub>73</sub> =0.032 K <sub>78</sub> =0.025 <b>K<sub>76</sub>=4.1</b> K <sub>128</sub> =0.05	K <sub>128</sub> =0.05 K <sub>112</sub> =0.08
Line-89	ABC G	B4, B8, B9	K <sub>43</sub> =0.099 K <sub>45</sub> =0.092 K <sub>49</sub> =0.094	K <sub>78</sub> =0.045 <b>K<sub>89</sub>=1.872</b>	K <sub>94</sub> =0.09 <b>K<sub>98</sub>=1.88</b>
Line-112	ABC G	B7, B11, B12,	K <sub>73</sub> =0.085 K <sub>78</sub> =0.095 K <sub>76</sub> =0.082 K <sub>128</sub> =0.09	<b>K<sub>112</sub>=2.6</b>	<b>K<sub>112</sub>=2.54</b> K <sub>128</sub> =0.07

### B. Grid-Tied Mode of Operation

Several cases have also been simulated for the grid-tied operation. The results for BCG fault at Line-37 of the microgrid are shown in Fig 9. The three buses with minimum PSV magnitude in this case are 7, 6 and 8 respectively. The FLI coefficients for the lines connected with these buses along with the current signal at PMU37 are shown in Fig. 10. The FLI coefficient of the faulty line i.e. Line-37 is greater than 1 while for healthy lines it is less than 1. Table IV reports the results for selected number of fault scenarios in the microgrid during the grid-tied mode of operation. To differentiate between the FLI coefficients of healthy and faulted line, the FLI coefficients for the faulted line are represented in bold letters. It can be observed from Table IV that the proposed scheme successfully detects and locates the faults in the grid-tied mode.

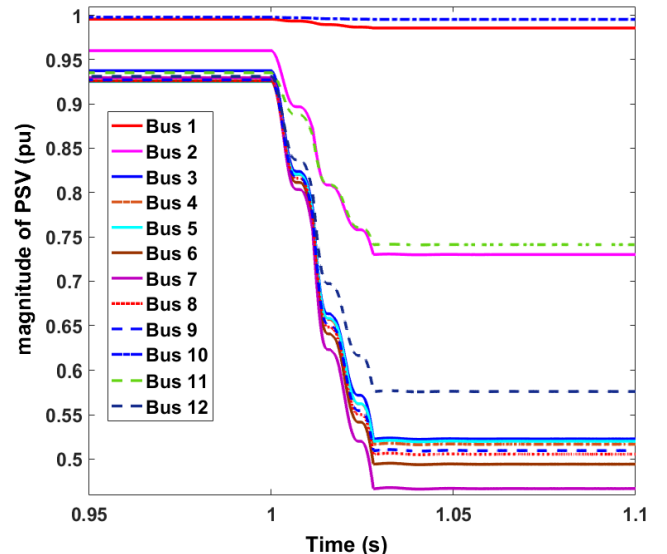


Fig. 9. Magnitude of PSVs at various buses when fault occurs at Line-37 of the microgrid working in grid-tied mode.

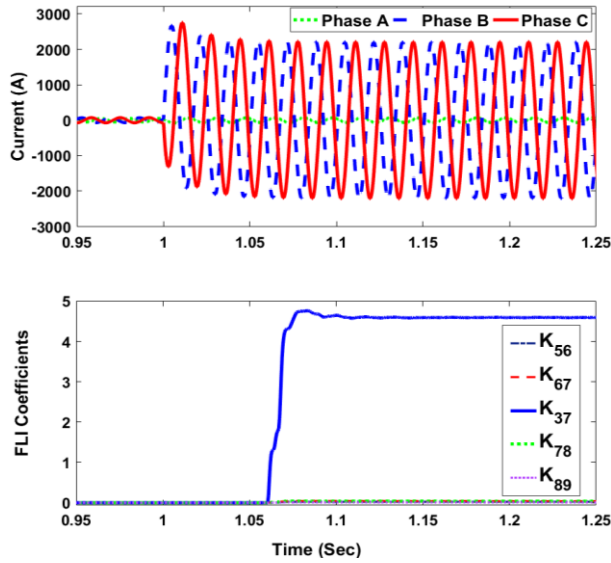


Fig. 10. Current signal and FLI coefficient at PMU37 for a BCG fault at line-37 of the grid-tied microgrid

TABLE IV

RESULTS FOR VARIOUS KIND OF FAULTS AT DIFFERENT LOCATIONS IN THE MICROGRID WORKING IN THE GRID-TIED MODE

Fault Location	Fault Type	FBI	$K_{xy}$ for Lines connected to Selected Buses		
			Bus-1	Bus-2	Bus-3
Line-45	AG	B3, B4, B5	$K_{32}=0.013$ $K_{34}=0.015$ $K_{37}=0.023$	$K_{43}=0.047$ <b><math>K_{45}=2.12</math></b> $K_{49}=0.089$	<b><math>K_{54}=2.22</math></b> $K_{56}=0.018$
Line-89	CG	B4, B8, B9	$K_{43}=0.025$ $K_{45}=0.032$ $K_{49}=0.014$	$K_{87}=0.041$ <b><math>K_{89}=1.83</math></b>	$K_{94}=0.091$ <b><math>K_{98}=1.81</math></b>
Line-34	ABG	B2, B3, B4	$K_{21}=0.009$ $K_{23}=0.045$	$K_{32}=0.048$ <b><math>K_{34}=2.45</math></b> $K_{37}=0.078$	<b><math>K_{43}=2.61</math></b> $K_{45}=0.025$ $K_{49}=0.061$
Line-67	BCG	B3, B6, B7	$K_{32}=0.048$ $K_{34}=0.012$ $K_{37}=0.049$	$K_{65}=0.042$ <b><math>K_{67}=4.10</math></b>	$K_{73}=0.025$ <b><math>K_{76}=4.01</math></b> $K_{78}=0.035$
Line-78	ABC	B6, B7, B8	$K_{32}=0.051$ $K_{34}=0.022$ $K_{37}=0.015$	$K_{65}=0.068$ $K_{67}=0.011$	$K_{73}=0.091$ <b><math>K_{78}=3.61</math></b> $K_{76}=0.041$
Line-23	ABC G	B2, B3, B7	$K_{21}=0.099$ <b><math>K_{23}=3.51</math></b>	<b><math>K_{32}=3.51</math></b> $K_{34}=0.029$ $K_{37}=0.045$	$K_{73}=0.058$ $K_{78}=0.072$ $K_{76}=0.078$

## V. POTENTIAL HARDWARE IMPLEMENTATION

To implement the proposed scheme, one can use the communication facilities of the smart grid. The developments in wireless communications provide standardized technologies for wide area and local area networks. The wireless communications has several advantages including high mobility, rapid deployment and low installation cost. Wireless signal transmission takes less than 0.1 ms for a distance up to 30km, which is acceptable for most distribution systems. In distribution networks, feeder is usually less than 20 km so, we can neglect the travelling time of electromagnetic wave along the line. Therefore, when a fault hits a feeder, the fault inception time appeared at each end of a line can be regarded as a same instant. The MPC can be implemented as a central processing unit and the proposed protection algorithm can be programmed in it. The hardware implementation of the proposed scheme will be considered in future study.

## VI. CONCLUSIONS

This paper proposed a centralized protection scheme for microgrids based on positive sequence complex power. A communication link is developed between the PMUs and MPC. The MPC processes the data to detect, locate and classify the faults in microgrids. To verify the efficacy of proposed scheme, several simulations were performed on a microgrid test system using MATLAB/SIMULINK software package. The results showed that the proposed scheme protected the grid-tied and the standalone microgrid against various faults. The advantages of the proposed scheme are as follows:

- The proposed scheme is based on sharing data from all buses in the microgrids.
- The proposed scheme uses only one relay instead of many standalone relays.
- No protection coordination issue.
- One and only one trip decision is issued from the microgrid protection commander.
- The relay has the characteristic of unit protection in distinguishing the faulted line.

The proposed protection scheme may leave the microgrid unprotected in case of communication failure. Therefore, a reliable communication channel is necessary for the proposed scheme.

## VII. ACKNOWLEDGMENT

This work was supported by the National Research Foundation of Korea (NRF) grant funded by the Korea government (MSIP) (No. 2015R1A2A1A10052459).

## VIII. REFERENCES

- [1] S. Mirsaedi, D. M. Said, M. W. Mustafa, M. H. Habibuddin, and K. Ghaffari, "Fault location and isolation in micro-grids using a digital central protection unit," *Renew. Sustain. Energy Rev.*, vol. 56, pp. 1–17, Apr. 2016.
- [2] M. A. Zamani, A. Yazdani, and T. S. Sidhu, "A Communication-Assisted Protection Strategy for Inverter-Based Medium-Voltage Microgrids," *IEEE Trans. Smart Grid*, vol. 3, no. 4, pp. 2088–2099, Dec. 2012.
- [3] S. Mirsaedi, D. Mat Said, M. Wazir Mustafa, M. Hafiz Habibuddin, and K. Ghaffari, "Progress and problems in micro-grid protection schemes," *Renew. Sustain. Energy Rev.*, vol. 37, pp. 834–839, Sep. 2014.
- [4] H. J. Laaksonen, "Protection principles for future microgrids," *IEEE Trans. Power Electron.*, vol. 25, no. 12, pp. 2910–2918, 2010.
- [5] H. Al-Nasseri, M. A. Redfern, and F. Li, "A voltage based protection for micro-grids containing power electronic converters," in *2006 IEEE Power Engineering Society General Meeting*, 2006, p. 7–pp.
- [6] S. A. Saleh, R. Ahshan, M. S. Abu-Khaizaran, B. Alsaid, and M. A. Rahman, "Implementing and testing-wpt-based digital protection for microgrid systems," *IEEE Trans. Ind. Appl.*, vol. 50, no. 3, pp. 2173–2185, 2014.
- [7] A. Oudalov and A. Fidigatti, "Adaptive network protection in microgrids," *Int. J. Distrib. Energy Resour.*, vol. 5, no. 3, pp. 201–226, 2009.
- [8] J. Ma, X. Wang, Y. Zhang, Q. Yang, and A. G. Phadke, "A novel adaptive current protection scheme for distribution systems with distributed generation," *Int. J. Electr. Power Energy Syst.*, vol. 43, no. 1, pp. 1460–1466, 2012.
- [9] S. Mirsaedi, D. M. Said, M. W. Mustafa, M. H. Habibuddin, and K. Ghaffari, "A Protection Strategy for Micro-Grids Based on Positive-Sequence Impedance," *Distrib. Gener. Altern. Energy J.*, vol. 31, no.

- 3, pp. 7–32, 2016.
- [10] S. Kar and S. R. Samantaray, “Time-frequency transform-based differential scheme for microgrid protection,” *IET Gener. Transm. Distrib.*, vol. 8, no. 2, pp. 310–320, Feb. 2014.
  - [11] E. Sortomme, S. S. Venkata, and J. Mitra, “Microgrid protection using communication-assisted digital relays,” *IEEE Trans. Power Deliv.*, vol. 25, no. 4, pp. 2789–2796, 2010.
  - [12] N. Jayawarna, C. Jones, M. Barnes, and N. Jenkins, “Operating microgrid energy storage control during network faults,” in *2007 IEEE International Conference on System of Systems Engineering, 2007*, pp. 1–7.
  - [13] M. A. Zamani, A. Yazdani, and T. S. Sidhu, “A control strategy for enhanced operation of inverter-based microgrids under transient disturbances and network faults,” *IEEE Trans. Power Deliv.*, vol. 27, no. 4, pp. 1737–1747, 2012.